

---

# Deriving Neural Network Design and Learning from the Probabilistic Framework of Chain Graphs

---

**Yuesong Shen**

Technical University of Munich, Germany  
yuesong.shen@tum.de

**Daniel Cremers**

Technical University of Munich, Germany  
cremers@tum.de

## Abstract

The last decade has witnessed a boom of neural network (NN) research and applications achieving state-of-the-art results in various domains. Yet, most advances on architecture and learning have been discovered empirically in a trial-and-error manner such that a more systematic exploration is difficult. Their theoretical analyses are limited and a unifying framework is absent. In this paper, we tackle this issue by identifying NNs as chain graphs (CGs) with chain components modeled as bipartite pairwise conditional random fields, and feed-forward as a form of approximate probabilistic inference. We show that from this CG interpretation we can systematically formulate an extensive range of the empirically discovered results, including various network designs (e.g., CNN, RNN, ResNet), activation functions (e.g., sigmoid, tanh, softmax, (leaky) ReLU) and regularizations (e.g., weight decay, dropout, BatchNorm). Furthermore, guided by this interpretation, we are able to derive “the preferred form” of residual block, recover the simple yet powerful IndRNN model and discover a new stochastic inference procedure: the partially collapsed feed-forward inference. We believe that our work can provide a well-founded formulation to analyze the nature and design of NNs, and can serve as a unifying theoretical framework for deep learning research.

## 1 Introduction

During the last decade, deep learning [13], the study of neural networks (NN), has achieved groundbreaking results in diverse areas such as computer vision [27, 56, 15, 34, 6], natural language processing [17, 62, 58, 9], generative modeling [24, 14] and reinforcement learning [36, 51], and various network designs have been proposed. However, neural network has been treated largely as a “black-box” function approximator, and its designs have chiefly been found via trial-and-error, with little or no theoretical justification. The absence of an underlying theoretical framework impairs our ability to understand the behavior of neural networks, to derive robustness guarantees, e.g., against adversarial attacks [55], and to perform guided searches of new designs and learning algorithms.

On the other hand, the well-established field of probabilistic graphical models [25] offers a solid theoretical framework that allows for flexible probabilistic modeling and natural handling of learning scenarios like generative modeling, unsupervised learning, domain knowledge integration, etc. However, haunted by intractable inference beyond simplistic structures and approximate methods with insufficient efficiency, its applicability to complex model design and large-scale data-driven learning is limited. While some more recent developments (e.g., [18, 45]) have been proposed to address this issue, the machine learning community has shifted its focus to deep learning approaches for their empirical effectiveness on large scale datasets.

While many existing machine learning models have corresponding graphical model interpretations [37], neural networks and graphical models have so far been treated as two distinct approaches.

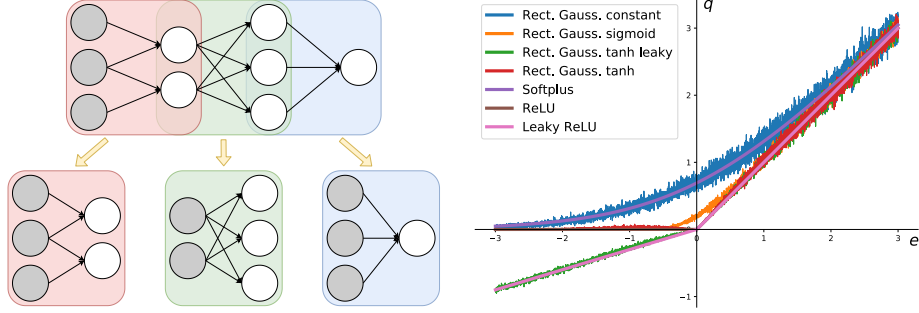


Figure 1: Neural networks can be interpreted as chain graphs where activation functions are determined by node distributions. *Left*: An example neural network interpreted as a chain graph with three chain components which represent its layers; *Right*: A variety of activation functions (softplus, ReLU, leaky ReLU) approximated by nodes following rectified Gaussian distributions ( $e, q$  as in Eq. (9)). We visualize the approximations stochastically by averaging over 200 samples.

Existing works that combine them [64, 6, 28] are limited to treat either neural networks as function approximators for amortized inference, or graphical models as post-processing steps.

In this paper, we show that a neural network can actually be interpreted as a special graphical model called chain graph (CG) [25], and feed-forward an efficient approximate probabilistic inference on it. Thus our work embeds deep learning research within the theoretical framework of graphical models, opening a path to a more systematic exploration of new architectures and learning strategies.

The remainder of the paper is organized as follows: We elucidate the link between neural networks and chain graphs in Section 2, covering core concepts within a simple binary sequential layer setting. In Section 3 we further discuss the chain graph interpretation in its generality, showing that it can cover an extensive range of existing designs. We then demonstrate by examples in Sections 4 and 5 how the proposed chain graph interpretation allows us to systematically design network structures and discover new learning approaches such as partially collapsed feed-forward. We then discuss related work in Section 6 and draw conclusions in Section 7.

## 2 Chain graph interpretation of neural networks

In this section we will derive a neural network formulation from a chain graph setting, thus providing a graphical model interpretation of neural networks. We will first consider the simpler case of a sequential structure and binary nodes, then extend to full generality in Section 3.

### 2.1 Chain graph representation

Consider a system represented by  $L$  layers of binary random variables  $X = (X^1, \dots, X^L)$ , where  $X_i^l$  is the  $i$ -th variable node in the  $l$ -th layer. Denote  $N^l$  the number of nodes in layer  $l$ , we assume that layers are homogeneous, i.e. nodes  $X_i^l$  in each layer  $l$  are of the same type: binary nodes taking value in  $\{\alpha^l, \beta^l\}$ . Similar to the sequential neural network setting,  $X^1$  has the role of representing the given input and  $X^L$  the output. In the discriminative learning context we model the conditional distribution  $P(X^2, \dots, X^L | X^1)$ . Making the assumption that this distribution can be represented by a chain graph [25] whose chain components represent layers  $X^l$  conditioned on their parent layer  $X^{l-1}$  (See Figure 1 Left for an example), it can then be factorized according to its chain components:

$$P(X^2, \dots, X^L | X^1) = \prod_{l=2}^L P(X^l | X^{l-1}). \quad (1)$$

To recover a typical neural network formulation, for each given chain component  $P(X^l | X^{l-1})$ , we further assume that it can be modeled by a bipartite pairwise conditional random field (CRF) [25]. Since the bipartite structure ensures the absence of intra-component connections between the nodes  $X_i^l$  in layer  $l$ , it leads to their conditional independence within the component and a node-wise factorization:  $P(X^l | X^{l-1}) = \prod_{i=1}^{N^l} P(X_i^l | X^{l-1})$ . If we express each node-wise factor  $P(X_i^l | X^{l-1})$

as a Gibbs distribution [25] parametrized by the (negative) unary/pairwise energies  $b_i^l$  and  $w_{j,i}^l$ , we have ( $Z_i^l(X^{l-1})$  are the partition functions that ensure normalized distributions):

$$P(X^l|X^{l-1}) = \prod_{i=1}^{N^l} P(X_i^l|X^{l-1}) = \prod_{i=1}^{N^l} \frac{1}{Z_i^l(X^{l-1})} \exp(b_i^l X_i^l + \sum_{j=1}^{N^{l-1}} w_{j,i}^l X_j^{l-1} X_i^l). \quad (2)$$

In the binary case, the normalization yields the following sigmoid function for each  $P(X_i^l|X^{l-1})$ :

$$P(X_i^l|X^{l-1}) = \sigma((2X_i^l - (\alpha^l + \beta^l))(b_i^l + (X^{l-1})^\top w_{\cdot,i}^l)). \quad (3)$$

## 2.2 Feed-forward as approximate probabilistic inference

Given the above chain graph representation and an input sample  $\tilde{x}^1$ , we consider the problem of inferring the marginal distribution  $Q_i^l$  of a node  $X_i^l$  and its expected value  $q_i^l$ , defined as

$$Q_i^l(x_i^l|\tilde{x}^1) = P(X_i^l = x_i^l|X^1 = \tilde{x}^1); \quad q_i^l = \mathbb{E}_{Q_i^l}[X_i^l] \quad (q^1 = \tilde{x}^1). \quad (4)$$

Then we have the following recursive expression of the marginal distributions  $Q$ :

$$Q_i^l(x_i^l|\tilde{x}^1) = \sum_{x^{l-1} \in \{\alpha^{l-1}, \beta^{l-1}\}^{N^{l-1}}} P(x_i^l|x^{l-1}) Q^{l-1}(x^{l-1}|\tilde{x}^1) = \mathbb{E}_{Q^{l-1}}[P(x_i^l|X^{l-1})]. \quad (5)$$

While  $P(x_i^l|x^{l-1})$  has a non-linear expression depicted in Eq (3), making the assumption that the pairwise weights are small ( $\|w_{\cdot,i}^l\| \ll 1$ ), we can make a first order (i.e. linear) approximation w.r.t.  $X^{l-1}$  and move the expectation inside, resulting in the following recursive approximation of  $q$ :

$$q_i^l = \sum_{x_i^l \in \{\alpha^l, \beta^l\}} x_i^l \mathbb{E}_{Q^{l-1}}[P(x_i^l|X^{l-1})] \approx \frac{\beta^l - \alpha^l}{2} \tanh\left(\frac{\beta^l - \alpha^l}{2} (b_i^l + (q^{l-1})^\top w_{\cdot,i}^l)\right) + \frac{\alpha^l + \beta^l}{2}. \quad (6)$$

The above expression is none other than a feed-forward process with a sigmoidal activation function. In particular, when  $\alpha^l = 0, \beta^l = 1$  we recover the sigmoid activation, and when  $\alpha^l = -1, \beta^l = 1$  we recover the tanh activation. Furthermore, the roles of  $\alpha^l$  and  $\beta^l$  are interchangeable.

We will see in Section 3 that nodes with different distributions  $P(x_i^l|x^{l-1})$  will lead to different activation functions, such as softmax, rectified linear unit (ReLU) or leaky ReLU. The generalization of this feed-forward approximation to other types of nodes is straightforward.

Now that we have the feed-forward update for  $q$ , learning can be conducted by maximizing the log-likelihood  $\log Q^L(\tilde{x}^L|\tilde{x}^1)$  of the ground-truth  $\tilde{x}^L$  with stochastic gradient descent.  $Q^L(\tilde{x}^L|\tilde{x}^1)$  can be computed from  $q^{L-1}$  via the same feed-forward linearization approximation applied to Eq. (5).

**When is the approximation accurate?** The approximation relies on the linearization (i.e. first order Taylor expansion) w.r.t.  $x^{l-1}$  to directly express  $q^l$  in terms of  $q^{l-1}$ . As discussed above, this approximation is accurate for small pairwise weights  $w^l$ . Alternatively, for piece-wise linear activation functions like ReLU, this assumption can be relaxed in all regions except around the kinks of the activation function. This might be a reason for their empirical superiority [38].

## 2.3 Soft clamping for compact input representation

Apart from using continuous input nodes (e.g., Gaussians) which would require input preprocessing, one can also directly represent continuous input values  $\tilde{x}_i^1$  defined over a range  $[\alpha^1, \beta^1]$  (such as pixel intensities) by binary nodes  $X^1$  and let  $\tilde{x}_i^1 = q_i^1 \in [\alpha^1, \beta^1]$ , meaning that we interpret input as observed expected values of the nodes  $X^1$  rather than their definite states. This justifies the direct usage of ranged input value for neural networks and is named ‘‘soft clamping’’ in Shen et al. [50].

## 3 Generality of the chain graph interpretation

In this section we show that the chain graph interpretation of neural networks in Section 2 can be generalized to cover an extensive range of existing NN designs (deep learning terminologies are marked in bold). Our discussion here mainly covers existing NN designs with direct interpretations in the CG framework. We complement this discussion in Sections 4 and 5 with examples of more elaborate or novel constructions, and believe that our framework can cover and inspire many more.

**Network architecture** The chain graph representation of neural networks allows for a general partially directed acyclic graph (PDAG) topology with modular chain components. This means that

- In terms of global network structure, we can construct multi-branched structures such as **inception modules** [56], or **residual blocks** [15, 16] as discussed in Section 4.1. Also, it is possible to build up **recurrent neural networks (RNNs)** for learning sequential data, as we will see in Section 4.2. Furthermore, the modularity of chain components justifies **transfer learning via partial reuse of pre-trained networks**, e.g., backbones trained for image classification can be reused for segmentation [6].
- In terms of layer structure within each chain component, the freedom to employ sparse connection patterns and shared/fixed parametrizations allows us to define layers beyond **dense connections** such as **convolution**, **average pooling** or **skip connection**. Moreover, the PDAG topology makes intra-layer connections possible: one can e.g., use a **non-bipartite CRF as the last layer**, which has been found beneficial for structured prediction tasks such as image segmentation [64, 6] or named entity recognition [28]. This would however require alternative inference procedures as feed-forward is no longer directly applicable.

**Activation function** Activation functions beyond **sigmoid** or **tanh** can be achieved with alternative node representations. In fact, a node  $X_i^l$  can follow a general distribution described by some features  $T^{l-1}(X_j^{l-1})$  of its parents  $X_j^{l-1}$  in layer  $l-1$  and a function  $f_i^l$  ensuring a valid distribution:

$$P(X_i^l | X^{l-1}) = f_i^l(X_i^l, e_i^l(T^{l-1}(X^{l-1}))) \quad (7)$$

$$\text{with } e_i^l(T^{l-1}(X^{l-1})) = b_i^l + \sum_{j=1}^{N^{l-1}} w_{j,i}^l T^{l-1}(X_j^{l-1}). \quad (8)$$

This results in the following general expression of the activation function for nodes  $X_i^l$  in layer  $l$  (using the feed-forward approximation discussed in Section 2.2):

$$q_i^l = \mathbb{E}_{Q_i^l}[T^l(X_i^l)] = \int_{x_i^l} T^l(x_i^l) \mathbb{E}_{Q^{l-1}}[P(x_i^l | X^{l-1})] dx_i^l \approx \int_{x_i^l} T^l(x_i^l) f_i^l(x_i^l, e_i^l(q^{l-1})) dx_i^l. \quad (9)$$

Concretely, linear Gaussian nodes result in the **identity activation** [25]. And multi-labeled nodes, specified as exponential families [25] with label indicators as features, lead to the **softmax activation**. Moreover, as shown by Figure 1 Right, a variety of activation functions can be approximated by the family of rectified Gaussian distributions, defined as ( $\mathcal{N}$  denotes the Gaussian distribution):

$$T_i^l(X_i^l) = X_i^l = \max(0, Y_i^l); \quad Y_i^l \sim \mathcal{N}(e_i^l(T^{l-1}(X^{l-1})), (s_i^l)^2). \quad (10)$$

In particular, with an appropriate constant standard deviation  $s_i^l = c$  (numerically evaluated to 1.776091849725427 to minimize the maximum pointwise approximation error), the rectified Gaussian can closely approximate the **softplus activation**.

Also, we find out that rectified Gaussian can approximate the **ReLU activation**, although our approach differs from other prior works: similar to the truncated Gaussian case [54], ReLU can be achieved with  $s_i^l = c \rightarrow 0$ , but this reduces to a deterministic setting; Nair and Hinton [38] propose a sigmoid-modulated standard deviation  $s_i^l = \sigma(e_i^l(T^{l-1}(X^{l-1})))$ , however it results in a curve between softplus and ReLU, as seen in Figure 1 Right. In lieu of these existing proposals, we find out that rectified Gaussian with tanh-modulated standard deviation

$$T_i^l(X_i^l) = X_i^l = \max(0, Y_i^l); \quad Y_i^l \sim \mathcal{N}(e_i^l(T^{l-1}(X^{l-1})), (\tanh(e_i^l(T^{l-1}(X^{l-1}))))^2) \quad (11)$$

serves a more accurate approximation. It can easily be extended to **leaky ReLU** with leak factor  $\epsilon$  by defining  $X_i^l = \max(\epsilon Y_i^l, Y_i^l)$  instead.

**Regularization** We complete this section with a brief review of some common NN regularization techniques: The small weight assumption made for the feed-forward approximation in Section 2.2 justifies weight regularizations such as **weight decay** beyond their general “anti-overfit” argument. Also, we note that normalization techniques such as **batch normalization** [22], **weight normalization** [47], **layer normalization** [3] and **group normalization** [59] can all be seen as reparametrizations of node distribution and fall within the general representation (Eq. (7)). Lastly, stochastic regularization with **dropout** [52] will be discussed in detail in Section 4.3, and in Section 5 we introduce a novel stochastic inference procedure called partially collapsed feed-forward.

## 4 Selected case studies of neural network designs

In light of the chain graph interpretation of neural networks, we reconsider several important aspects of neural network designs in this section: We start in Section 4.1 with the residual block [15], an effective structure to scale up networks in depth, and provide a formulation that leads to its revised pre-activation variant [16]; Then in Section 4.2 we examine the sequential data learning scenario with RNNs, deriving first the standard simple recurrent network (SRN) and then, with careful consideration of independence assumptions, recover a simple yet powerful variant called independently RNN (IndRNN) [31]; Lastly in Section 4.3, we consider stochastic regularization with dropout [52]. We continue in Section 5 with a novel proposal called partially collapsed feed-forward.

### 4.1 Going deeper: residual block as refinement module

Since the introduction of residual network (ResNet) [15], residual block has shown to be effective for building up very deep networks that achieve state-of-the-art results for tasks like image classification [15], image segmentation [6] and speech recognition [62]. Here we show that it can be interpreted as a refinement module. Interestingly, our chain graph based interpretation recovers the pre-activation variant, which has been shown empirically by He et al. [16] to be the preferred choice.

Given a base module with input  $X^i$  and output  $X^o$ , the construct of residual block can be seen as a refinement module defined over the base submodule and a refining submodule: the base submodule from  $X^i$  to  $X^o$  is augmented with a side chain that puts in sequence a copy of the base submodule from  $X^i$  to  $\tilde{X}^o$  (with shared weight and identical structure w.r.t the base module) and a refining submodule from  $\tilde{X}^o$  to  $X^o$ . Figure 2 shows an example refinement module with base submodule  $X^{l-1} \rightarrow X^l$  and refining submodule  $\tilde{X}^l \rightarrow Z^l \rightarrow X^l$ , with its chain graph representation on the left and the corresponding computational graph on the right.

One remarkable fact is that the refinement process can be recursive: the base submodule itself can also be a refinement module. In terms of computational graph, this results in a chained sequence of residual blocks. Also, the refinement submodule can have an arbitrary structure (e.g., bottleneck [15] or ResNeXt [61]), except that its input  $\tilde{X}^o$  and output  $X^o$  must have identical shape and type.

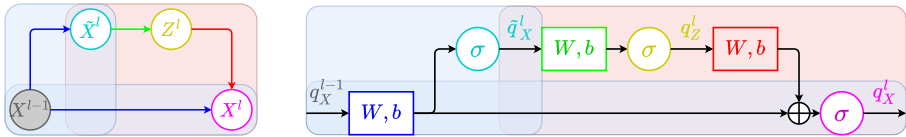


Figure 2: Example of a refinement module (left) and its corresponding computational graph (right), composed of a base submodule  $X^{l-1} \rightarrow X^l$  (blue background) and a refining submodule  $\tilde{X}^l \rightarrow Z^l \rightarrow X^l$  (red background). In the computational graph each  $W, b$  represents a linear connection (Eq. (8)) and  $\sigma$  an activation function. Same color identifies corresponding parts in the two graphs. We see that refinement modules correspond exactly to pre-activation residual blocks.

Noteworthy, we observe that our refinement module derivation directly leads to the improved pre-activation variant of ResNet [16], originally found via trial-and-error among a list of proposed variants. The authors show empirically that this form can benefit from 1000+ layers while the original form yields worse results compared to using a bit more than 100 layers. We refer readers who are interested in experimental validation on vision tasks to this paper.

### 4.2 Learning sequential data

In contrast to the usual i.i.d. assumption made among entries of a dataset, sequential data introduce temporal dependencies among entries within each sequence. To explicitly express these dependencies, we denote  $\tilde{X}^{l,t}$  the random variables in layer  $l$  at time  $t$  and  $\tilde{x}^{1,t}$  the input at time  $t$ . A deep learning solution for learning sequential data is the recurrent neural network [13], where hidden states are introduced to summarize previous time steps. Here we investigate it in depth, starting with the chain graph representation of simple recurrent network in Section 4.2.1 and going further in Section 4.2.2, rediscovering the independently RNN [31] via careful reconsideration of independence assumptions.

#### 4.2.1 Chain graph representation of simple recurrent network

Processing sequential data requires modification of the chain components: making the Markov assumption, a chain component at time  $t$  should model  $P(X^{l,t}|X^{l-1,t}, X^{l,t-1})$ , taking input both from parent layer(s) ( $X^{l-1,t}$ ) and previous time step ( $X^{l,t-1}$ ). We can recover a simple recurrent network by making dense pairwise connections from  $X^{l,t-1}$  to  $X^{l,t}$  within each corresponding chain component of its recurrent layers. For the non-recurrent layers we simply assume  $P(X^{l,t}|X^{l-1,t}, X^{l,t-1}) = P(X^{l,t}|X^{l-1,t})$ , i.e., no direct dependency of the previous time step.

Unfortunately, the SRN is known to suffer from vanishing / exploding gradient and can not handle long sequences. Existing works, such as the commonly used long-short term memory (LSTM) [20] or the gated recurrent unit (GRU) [8], remedy this issue via long term memory cells and gating. However, they tend to result in bloated structures, and still cannot handle very long sequences [31].

#### 4.2.2 Independently RNN: rethinking the simple recurrent network

While dense connections provide comprehensive parametrizations, the success of convolutional neural networks demonstrates that reasonable sparse connections can result in superior performance. Returning to the SRN case, since the entries  $\{X_i^{l,t}\}_{i \in [1..N^l]}$  within the  $l$ -th component are conditionally independent at each time step  $t$ , it is actually logical to assume that they are also not directly dependent through time, i.e.,  $P(X_i^{l,t}|X^{l-1,t}, X^{l,t-1}) = P(X_i^{l,t}|X^{l-1,t}, X_i^{l,t-1})$ . This further assumption in fact leads to the variant called independently RNN [31], illustrated in Figure 3.

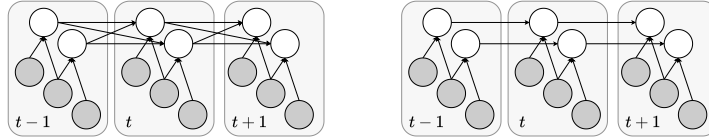


Figure 3: Example comparison of an SRN (left) recurrent layer v.s. an IndRNN (right) recurrent layer. IndRNN, the better variant, enforces the conditional independence between nodes through time.

While simpler, Li et al. [31, 32] have shown empirically that IndRNN significantly outperforms not only SRN, but also LSTM-based variants: it can process much longer sequences and make use of the ReLU activation and residual blocks to build up deep RNNs whose depth is seemingly only limited by hardware capacity. We refer readers seeking experimental validation to their work.

### 4.3 Stochastic regularization with dropout

Dropout [52] is a practical stochastic regularization method widely used especially for regularizing dense layers. Its introduction of stochastic noise has shown effective at regularizing neural networks and its success can also be argued from an ensemble learning perspective [52]. Here we formulate and analyze dropout from a chain graph perspective in Section 4.3.1. Moreover, in view of the chain graph interpretation, we will then devise a novel stochastic inference procedure called partially collapsed feed-forward in Section 5, followed by experimental evaluations in Section 5.1.

#### 4.3.1 Chain graph representation of dropout

For a chain component from  $X^{l-1}$  to  $X^l$ , we introduce for each input entry  $X_j^{l-1}$  a corresponding Bernoulli auxiliary variable  $D_j^{l-1} \sim \text{Bernoulli}(p^{l-1})$  taking value from  $\{0, 1\}$ . Furthermore, each pairwise factor connecting  $X_j^{l-1}$  and  $X_i^l$  is augmented to ternary with the inclusion of  $D_j^{l-1}$ , and in general for each augmented chain component we represent its node-wise conditional probability as

$$P(X_i^l|X^{l-1}, D^{l-1}) = f_i^l(X_i^l, e_i^l(T^{l-1}(X^{l-1}), D^{l-1})) \quad (12)$$

$$\text{with } e_i^l(T^{l-1}(X^{l-1}), D^{l-1}) = b_i^l + \sum_{j=1}^{N^{l-1}} D_j^{l-1} w_{j,i}^l T^{l-1}(X_j^{l-1}). \quad (13)$$

The behavior of dropout is reproduced as follows: during training we sample  $D^{l-1}$  during each feed-forward inference, while at test time we marginalize instead, resulting in the constant scaling of  $p^{l-1}$ . One can also use other noise distributions such as Gaussian [52].

## 5 Partially collapsed feed-forward

Instead of using dedicated noise sources as in dropout, stochastic behavior can simply be achieved via sampling: In our case, forward sampling (also called ancestral sampling) [25] can be performed conditioned on the input nodes which are ancestral nodes. This process generates unbiased samples, and for each generation only requires a single pass of the network. Thus it can be seen as a stochastic counterpart of feed-forward that offers unbiased estimates at the cost of stochasticity.

However, directly replacing feed-forward with forward sampling can cause issues: Apart from high variance, sampling hinders the gradient flow of backpropagation during parameter update. While for many continuous random variables the reparameterization trick [24] can maintain the gradient flow, for discrete variables this is not applicable. To solve this problem in the general case, we propose to simply “mix up” feed-forward and forward sampling: in each forward inference during training, we randomly select a part of nodes to sample and the rest to compute in closed-form as in a normal feed-forward. Thus for a node  $X_i^l$ , we have

$$q_i^l = \begin{cases} E_{Q_i^l}[T^l(X_i^l)] & \text{if collapsed (feed-forward);} \\ T^l(x_i^l), x_i^l \sim Q_i^l & \text{if uncollapsed (forward sampling).} \end{cases} \quad (14)$$

Following the collapsed sampling [25] terminology, we call this the partially collapsed feed-forward (PCFF), generalizing over feed-forward and forward sampling as its fully collapsed / uncollapsed extremes. The partial collapsing ensures the gradient flow. It also provides a bias–variance trade-off.

### 5.1 Experimental evaluations of partially collapsed feed-forward

To evaluate the empirical performance of partially collapsed feed-forward, we conduct a series of experiments. Our emphasis here is to understand the behavior of PCFF under various contexts and not to achieve best result for any specific task. We only use components with previously discussed chain graph interpretation, and we adopt the reparameterization trick [24] for ReLU PCFF samples.

The following experiments show that PCFF is overall an effective stochastic regularization method. Compared to dropout, it tends to produce more consistent performance improvement, and is comparable to dropout in cases where dropout also works. Thus PCFF is a viable alternative to dropout.

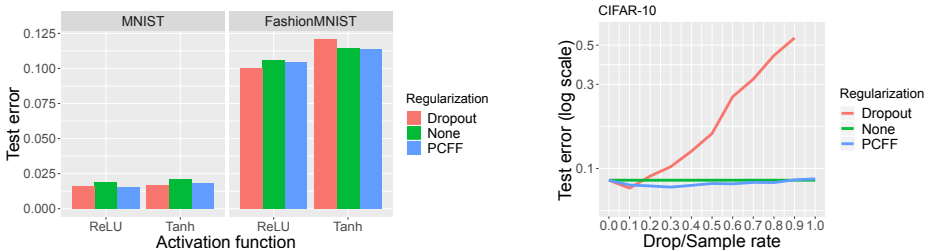


Figure 4: Comparison of stochastic methods (None/Dropout/PCFF) in terms of image classification test errors (lower is better) under various settings. Left: MNIST/FashionMNIST datasets with a simple dense network and tanh/ReLU activation functions; Right: CIFAR-10 dataset with ResNet20 and varying drop/sample rates. All reported results are average values of three runs. Compared to dropout, PCFF can achieve comparable results, and tend to deliver more consistent improvements.

**Simple dense network** We start with a simple network with two dense hidden layers of 1024 nodes to classify MNIST [29] and FashionMNIST [60] images<sup>1</sup>. We use PyTorch [43], train with stochastic gradient descent (learning rate 0.01, momentum 0.9), and set up 20% of training data as validation set for performance monitoring and early-stopping. We set drop rate to 0.5 for dropout, and for PCFF we set the sampling rate to 0.4 for tanh and 1.0 (full sampling) for ReLU. Figure 4 Left reports the test errors with different activation functions and stochastic regularizations.

We see that dropout and PCFF are overall comparable, and both improve the results in most cases. Also, the ReLU activation consistently produces better results than tanh. Additional experiments show that PCFF and dropout can be used together, which sometimes further improves the performance.

<sup>1</sup>Implementation available at: <https://github.com/tum-vision/nascg>

**Convolutional residual network** To figure out the applicability of PCFF in convolutional residual networks, we experiment on CIFAR-10 [26] image classification. For this we adapt an existing implementation [21] to use the pre-activation variant. We focus on the ResNet20 structure, and follow the original learning rate schedule except for setting up a validation set of 10% training data to monitor training performance. Figure 4 Right summarizes the test errors under different settings.

We observe that in this case PCFF can improve the performance over a wide range of sampling rates, while dropout is only effective with drop rate 0.1, and large drop rates in this case significantly deteriorate the performance. We also observe a clear trade-off of the PCFF sampling rate, where a partial sampling of 0.3 yields the best result.

**Independently RNN** We complete our experimental evaluations on PCFF with an RNN test case. For this we used IndRNNs with 6 layers to solve the sequential/permuted MNIST classification problem based on an existing Implementation<sup>2</sup> provided by the authors of IndRNN [31, 32]. We tested over dropout with drop rate 0.1 and PCFF with sample rate 0.1 and report the average test accuracy of three runs. We notice that, while in the permuted MNIST case both dropout (0.9203) and PCFF (0.9145) improves the result (0.9045), in the sequential MNIST case, dropout (0.9830) seems to worsen the performance (0.9841) whereas PCFF (0.9842) delivers comparable result.

## 6 Related work

Beyond the universal function approximator theory [13], existing works have attempted to connect deep learning to other theoretical frameworks to analyze its underlying mechanism. One line of research studies neural networks with infinite width and has shown their equivalence to Gaussian processes [41, 30], enabling the kernel method analysis [23]. Others have examined the signal propagation on untrained neural networks with random weights [44, 49]. Also, optimal transport has been used to analyze deep generative models [2, 12]. While these theories lead to interesting findings, they are however derived under limited or unrealistic settings, and can not provide a unifying theoretical framework for the existing deep learning research.

Alternatively, some existing works study the post-hoc interpretability [33], proposing methods to analyze the empirical behavior of trained neural networks: activation maximization [10], typical input synthesis [42], deconvolution [63], layer-wise relevance propagation [4], etc. These methods can offer valuable insights to the practical behavior of neural networks, however they represent distinct approaches and focuses, and are all limited within the universal function approximator view.

From the graphical model community, there are also efforts to construct hierarchical models for data-driven learning problems, such as sigmoid belief network [40], deep belief network [19], deep Boltzmann machine [46] and sum product network [45]. These models have shown promising potentials for e.g., generative modeling and unsupervised learning. Nevertheless, they are yet to rival neural network for discriminative learning, both in performance and efficiency.

Lastly, the relation between neural network and graphical model has been intuitively hinted here and there in the deep learning literatures (e.g., [13]). Especially, neural networks are sometimes treated as graphical models with deterministic hidden nodes [5], which is however an atypical degenerate regime. To the best of our knowledge, our work provides the first rigorous and comprehensive formulation and analysis of the (non-degenerate) graphical model interpretation of neural networks.

## 7 Conclusion

In this work, we show that neural networks can be interpreted as chain graphs with bipartite pairwise CRF components, and that feed-forward can be regarded as an approximate inference procedure. We also demonstrate that the chain graph interpretation covers an extensive range of existing network structures. It clarifies the underlying mechanism and assumptions made during the modeling and learning process, offering guidance to design choices and discovery of new approaches. While our discussion here is inevitably non-exhaustive, we believe the proposed chain graph framework can encompass and inspire many more, serving as a solid foundation for deep learning research to come.

---

<sup>2</sup>[https://github.com/Sunnydreamrain/IndRNN\\_pytorch](https://github.com/Sunnydreamrain/IndRNN_pytorch)



## Broader Impact

As our work provides a formulation for the underlying mechanism of neural networks, it can facilitate the research on the explainability of deep learning systems. This is important for developing AIs with safety guarantee and decision transparency [48], which is critical for applications such as medical diagnosis or autonomous driving, and assures compliance to regulations (e.g., GDPR [11]) and necessary standards for proper usage.

Furthermore, our work can encourage a transition from trial-and-error to a more systematic and theoretically grounded exploration of new deep learning models and learning strategies. This can save a fair amount of computationally-heavy training and testing [53], contributing to energy saving and climate protection [39].

In general, this work can potentially accelerate the deep learning research and would benefit all machine learning researchers and AI users. However, it can also lead to faster development of misused AI if uncontrolled, causing deceit [7], discrimination [1], unemployment [57] and disaster [35].

## Acknowledgments and Disclosure of Funding

We would like to thank Tao Wu and Florian Bernard for helpful discussions and proofreadings. This work was supported by the ERC Grant 3DReloaded and by the Munich Center for Machine Learning.

## References

- [1] Computer programs recognise white men better than black women. *The Economist*, 2018. Retrieved from <https://www.economist.com/science-and-technology/2018/02/15/computer-programs-recognise-white-men-better-than-black-women>.
- [2] M. Arjovsky, S. Chintala, and L. Bottou. Wasserstein generative adversarial networks. In *ICML*, 2017.
- [3] L. J. Ba, J. R. Kiros, and G. E. Hinton. Layer normalization. *CoRR*, abs/1607.06450, 2016.
- [4] S. Bach, A. Binder, G. Montavon, F. Klauschen, K.-R. Müller, and W. Samek. On pixel-wise explanations for non-linear classifier decisions by layer-wise relevance propagation. *PLOS ONE*, 10(7):1–46, 07 2015.
- [5] W. L. Buntine. Operations for learning with graphical models. *J. Artif. Int. Res.*, 2(1):159–225, Dec. 1994.
- [6] L. Chen, G. Papandreou, I. Kokkinos, K. Murphy, and A. L. Yuille. Deeplab: Semantic image segmentation with deep convolutional nets, atrous convolution, and fully connected crfs. *TPAMI*, 40(4):834–848, 2018.
- [7] R. Chesney and D. Citron. Deep Fakes: A Looming Crisis for National Security, Democracy and Privacy? *The Lawfare Blog*, 2018. Retrieved from <https://www.lawfareblog.com/deep-fakes-looming-crisis-national-security-democracy-and-privacy>.
- [8] K. Cho, B. van Merriënboer, C. Gulcehre, D. Bahdanau, F. Bougares, H. Schwenk, and Y. Bengio. Learning phrase representations using RNN encoder–decoder for statistical machine translation. In *EMNLP*, 2014.
- [9] J. Devlin, M.-W. Chang, K. Lee, and K. Toutanova. BERT: Pre-training of deep bidirectional transformers for language understanding. In *NAACL*, 2019.
- [10] D. Erhan, Y. Bengio, A. Courville, and P. Vincent. Visualizing higher-layer features of a deep network. 2009.
- [11] European Parliament and Council of the European Union. Regulation (EU) 2016/679 of the European Parliament and of the Council of 27 April 2016 on the protection of natural persons with regard to the processing of personal data and on the free movement of such data, and repealing Directive 95/46/EC (General Data Protection Regulation) (Text with EEA relevance), 2016.
- [12] A. Genevay, G. Peyré, and M. Cuturi. GAN and VAE from an optimal transport point of view. *arXiv preprint arXiv:1706.01807*, 2017.
- [13] I. Goodfellow, Y. Bengio, and A. Courville. *Deep Learning*. MIT Press, 2016.
- [14] I. J. Goodfellow, J. Pouget-Abadie, M. Mirza, B. Xu, D. Warde-Farley, S. Ozair, A. Courville, and Y. Bengio. Generative adversarial networks. In *NIPS*, 2014.

- [15] K. He, X. Zhang, S. Ren, and J. Sun. Deep residual learning for image recognition. In *CVPR*, 2016.
- [16] K. He, X. Zhang, S. Ren, and J. Sun. Identity mappings in deep residual networks. In *ECCV*, 2016.
- [17] G. Hinton, L. Deng, D. Yu, G. E. Dahl, A. Mohamed, N. Jaitly, A. Senior, V. Vanhoucke, P. Nguyen, T. N. Sainath, and B. Kingsbury. Deep neural networks for acoustic modeling in speech recognition: The shared views of four research groups. *IEEE Signal Processing Magazine*, 29(6):82–97, 2012.
- [18] G. E. Hinton. Training products of experts by minimizing contrastive divergence. *Neural Comput.*, 14(8): 1771–1800, Aug. 2002.
- [19] G. E. Hinton, S. Osindero, and Y.-W. Teh. A fast learning algorithm for deep belief nets. *Neural Comput.*, 18(7):1527–1554, 2006.
- [20] S. Hochreiter and J. Schmidhuber. Long short-term memory. *Neural Comput.*, 9(8):1735–1780, Nov. 1997.
- [21] Y. Idelbayev. Proper ResNet implementation for CIFAR10/CIFAR100 in PyTorch. [https://github.com/akamaster/pytorch\\_resnet\\_cifar10](https://github.com/akamaster/pytorch_resnet_cifar10). Accessed: 2020-06-05.
- [22] S. Ioffe and C. Szegedy. Batch normalization: Accelerating deep network training by reducing internal covariate shift. In *ICML*, 2015.
- [23] A. Jacot, F. Gabriel, and C. Hongler. Neural tangent kernel: Convergence and generalization in neural networks. In *NeurIPS*, 2018.
- [24] D. P. Kingma and M. Welling. Auto-encoding variational bayes. In *ICLR*, 2014.
- [25] D. Koller and N. Friedman. *Probabilistic Graphical Models: Principles and Techniques*. MIT Press, 2009.
- [26] A. Krizhevsky. Learning multiple layers of features from tiny images. Technical report, 2009.
- [27] A. Krizhevsky, I. Sutskever, and G. E. Hinton. ImageNet classification with deep convolutional neural networks. In *NIPS*, 2012.
- [28] G. Lample, M. Ballesteros, S. Subramanian, K. Kawakami, and C. Dyer. Neural architectures for named entity recognition. In *NACCL*, 2016.
- [29] Y. Lecun, L. Bottou, Y. Bengio, and P. Haffner. Gradient-based learning applied to document recognition. *Proceedings of the IEEE*, 86(11):2278–2324, 1998.
- [30] J. Lee, Y. Bahri, R. Novak, S. S. Schoenholz, J. Pennington, and J. Sohl-Dickstein. Deep neural networks as gaussian processes. In *ICLR*, 2018.
- [31] S. Li, W. Li, C. Cook, C. Zhu, and Y. Gao. Independently recurrent neural network (indrnn): Building a longer and deeper RNN. In *CVPR*, 2018.
- [32] S. Li, W. Li, C. Cook, Y. Gao, and C. Zhu. Deep independently recurrent neural network (indrnn). *arXiv preprint arXiv:1910.06251*, 2019.
- [33] Z. C. Lipton. The mythos of model interpretability. *Commun. ACM*, 61(10):36–43, Sept. 2018.
- [34] J. Long, E. Shelhamer, and T. Darrell. Fully convolutional networks for semantic segmentation. In *CVPR*, 2015.
- [35] M. McFarland. ‘Slaughterbots’ film shows potential horrors of killer drones. CNN, 2017. Retrieved from <https://money.cnn.com/2017/11/14/technology/autonomous-weapons-ban-ai/index.html>.
- [36] V. Mnih, K. Kavukcuoglu, D. Silver, A. A. Rusu, J. Veness, M. G. Bellemare, A. Graves, M. Riedmiller, A. K. Fidjeland, G. Ostrovski, S. Petersen, C. Beattie, A. Sadik, I. Antonoglou, H. King, D. Kumaran, D. Wierstra, S. Legg, and D. Hassabis. Human-level control through deep reinforcement learning. *Nature*, 518(7540):529–533, Feb. 2015.
- [37] K. P. Murphy. *Machine Learning: A Probabilistic Perspective*. MIT Press, 2012.
- [38] V. Nair and G. E. Hinton. Rectified linear units improve restricted boltzmann machines. In *ICML*, 2010.
- [39] J. Naughton. Can the planet really afford the exorbitant power demands of machine learning? The Guardian, 2019. Retrieved from <https://www.theguardian.com/commentisfree/2019/nov/16/can-planet-afford-exorbitant-power-demands-of-machine-learning>.

- [40] R. M. Neal. Connectionist learning of belief networks. *AI*, 56(10):71–113, July 1992.
- [41] R. M. Neal. *Bayesian Learning for Neural Networks*. Springer-Verlag, 1996.
- [42] A. Nguyen, A. Dosovitskiy, J. Yosinski, T. Brox, and J. Clune. Synthesizing the preferred inputs for neurons in neural networks via deep generator networks. In *NIPS*, 2016.
- [43] A. Paszke, S. Gross, S. Chintala, G. Chanan, E. Yang, Z. DeVito, Z. Lin, A. Desmaison, L. Antiga, and A. Lerer. Automatic differentiation in pytorch. In *NIPS-W*, 2017.
- [44] B. Poole, S. Lahiri, M. Raghu, J. Sohl-Dickstein, and S. Ganguli. Exponential expressivity in deep neural networks through transient chaos. In *NIPS*, 2016.
- [45] H. Poon and P. Domingos. Sum-product networks: A new deep architecture. In *UAI*, 2011.
- [46] R. Salakhutdinov and G. Hinton. An efficient learning procedure for deep boltzmann machines. *Neural Comput.*, 24(8):1967–2006, Aug. 2012.
- [47] T. Salimans and D. P. Kingma. Weight normalization: A simple reparameterization to accelerate training of deep neural networks. In *NIPS*. 2016.
- [48] I. Sample. Computer says no: why making AIs fair, accountable and transparent is crucial. The Guardian, 2017. Retrieved from <https://www.theguardian.com/science/2017/nov/05/computer-says-no-why-making-ais-fair-accountable-and-transparent-is-crucial>.
- [49] S. S. Schoenholz, J. Gilmer, S. Ganguli, and J. Sohl-Dickstein. Deep information propagation. In *ICLR*, 2017.
- [50] Y. Shen, T. Wu, C. Domokos, and D. Cremers. Probabilistic discriminative learning with layered graphical models. *CoRR*, abs/1902.00057, 2019.
- [51] D. Silver, A. Huang, C. J. Maddison, A. Guez, L. Sifre, G. van den Driessche, J. Schrittwieser, I. Antonoglou, V. Panneershelvam, M. Lanctot, S. Dieleman, D. Grewe, J. Nham, N. Kalchbrenner, I. Sutskever, T. Lillicrap, M. Leach, K. Kavukcuoglu, T. Graepel, and D. Hassabis. Mastering the game of Go with deep neural networks and tree search. *Nature*, 529(7587):484–489, Jan. 2016.
- [52] N. Srivastava, G. Hinton, A. Krizhevsky, I. Sutskever, and R. Salakhutdinov. Dropout: A simple way to prevent neural networks from overfitting. *JMLR*, 15(56):1929–1958, 2014.
- [53] E. Strubell, A. Ganesh, and A. McCallum. Energy and policy considerations for deep learning in NLP. In *ACL*, 2019.
- [54] Q. Su, X. Liao, C. Chen, and L. Carin. Nonlinear statistical learning with truncated gaussian graphical models. In *ICML*, 2016.
- [55] C. Szegedy, W. Zaremba, I. Sutskever, J. Bruna, D. Erhan, I. J. Goodfellow, and R. Fergus. Intriguing properties of neural networks. In *ICLR*, 2014.
- [56] C. Szegedy, Wei Liu, Yangqing Jia, P. Sermanet, S. Reed, D. Anguelov, D. Erhan, V. Vanhoucke, and A. Rabinovich. Going deeper with convolutions. In *CVPR*, 2015.
- [57] M. Y. Vardi. Are robots taking our jobs? The Conversation, 2016. Retrieved from <https://theconversation.com/are-robots-taking-our-jobs-56537>.
- [58] A. Vaswani, N. Shazeer, N. Parmar, J. Uszkoreit, L. Jones, A. N. Gomez, Ł. Kaiser, and I. Polosukhin. Attention is all you need. In *NIPS*, 2017.
- [59] Y. Wu and K. He. Group normalization. In *ECCV*, 2018.
- [60] H. Xiao, K. Rasul, and R. Vollgraf. Fashion-mnist: a novel image dataset for benchmarking machine learning algorithms. *CoRR*, abs/1708.07747, 2017.
- [61] S. Xie, R. B. Girshick, P. Dollár, Z. Tu, and K. He. Aggregated residual transformations for deep neural networks. In *CVPR*, 2017.
- [62] W. Xiong, J. Droppo, X. Huang, F. Seide, M. L. Seltzer, A. Stolcke, D. Yu, and G. Zweig. Toward human parity in conversational speech recognition. *IEEE/ACM Trans. Audio, Speech and Lang. Proc.*, 25(12): 2410–2423, Dec. 2017.
- [63] M. D. Zeiler and R. Fergus. Visualizing and understanding convolutional networks. In *ECCV*, 2014.
- [64] S. Zheng, S. Jayasumana, B. Romera-Paredes, V. Vineet, Z. Su, D. Du, C. Huang, and P. H. S. Torr. Conditional random fields as recurrent neural networks. In *ICCV*, 2015.